NHDOT SPR2 PROGRAM
RESEARCH PROGRESS REPORT

INSTRUCTIONS:
Project Managers and/or research project investigators should complete a progress report at least every three months during the project duration. Reports are due the 5th of the month following the end of the quarter. Please provide a project update even if no work was done during this reporting period.

Project # 26962M	**Report Period** Year: 2018 ☐ Q1 (Jan-Mar) ☐ Q2 (Apr-Jun) X Q3 (Jul-Sep) ☐ Q4 (Oct-Dec)	
Project Title: Evaluation of Gusset-less Truss Connection to Aid Bridge Inspection and Condition Assessment		
Project Investigator: Erin S. Bell Co-Project Investigator: Ricardo A. Medina **Phone: (603)862-3850** **E-mail: erin.bell@unh.edu**		
Research Start Date: December 15, 2016	**Research End Date:** December 31, 2018	**Project schedule status:** ☐ On schedule ☐ Ahead of schedule X Behind schedule

Brief Project Description:

The Memorial Bridge connecting Portsmouth, NH and Kittery, ME was re-opened to traffic in 2013. One of the major innovations of the reconstructed bridge is the first ever gusset-less truss connection in a vehicular bridge in the United States. Traditional gusset plates are the most vulnerable element in a truss-bridge structure and a source of significant cost, effort, and concern for bridge managers and owners. The goal of the proposed research is to integrate field-collected performance data, laboratory experimental testing, and physics-based structural modeling to develop a protocol to assess the condition and predict the remaining life of the gusset-less truss connections used at the Memorial Bridge. It is anticipated that the aforementioned approach will be modified to develop a framework to extend this protocol for application to future innovative structural elements.

The objectives of this project are to:

- Original Objective: Create two specimen pairs (A and B) of a scale model of a gusset-less connection from the Memorial Bridge. Specimen pair A (top chord connection) will be tested to failure in a quasi-static testing protocol and Specimen pair B (bottom chord connection) will be tested for fatigue performance. Modified Objective: Create two specimens that are a scaled model of the gusset-less connection from the Memorial Bridge focused on the bend radius weld section of the connection.
- Conduct quasi-static set of tests on each member of Specimen A to determine stress distribution in the connection.
- Evaluate these results in conjunction with field collected data and analytical models that are the work product of a complimentary FHWA-AID DEMO project to: (i) further understand and quantify the structural performance of the gusset-less connection, and (ii) validate analytical models.
- Conduct fatigue testing on Specimen pair B and collect performance data to determine the stress pattern and predict fatigue failure mode.
- Compare the findings of this project with the FHWA guideline for connection assessment to facilitate the development of an evaluation protocol for inspection and structural condition assessment.

Progress this Quarter (include meetings, installations, equipment purchases, significant progress, etc.):

Complete Literature Review and Finalize Testing Plan

These tasks were completed during the last quarter of 2017 and first quarter of 2018.

Design and Construction of Scale Models

During the second quarter of 2017, weld specimens with and without defects were fabricated to evaluate the fatigue performance of intact and defective 7/16" welds (see Figure 1). As part of this effort, a mock test was performed. Due to limitations of the testing machine, significant slippage was present during the cyclic test and an alternative testing approach was designed. The Civil and Environmental Engineering Department procured grips to be attached to the Instron Universal Testing Machine at the UNH Structural Engineering Laboratory. The advantage of using the aforementioned grips is twofold: (i) the grips prevents any slippage in the response once the specimens are exposed to cyclic loading, and (ii) time and resources are saved given that specimens do not need to be machined to a circular cross-section and specimens with square cross-sections can be tested without modifications. Figure 1 shows one of the specimens to be tested. The only machining necessary involved reducing the cross-section in the middle of the specimen (where the weld is located) in order to induce fatigue failure at this location. The grips arrived toward the end of the third quarter and testing in October and November demonstrated that they were defective. Material Testing Technology (MTT) were contacted, and after a few weeks going back and forth with them, the original grips were returned, and a new set of grips were sent to us at the beginning of December. Further delays related to the testing apparatus have delayed the coupon testing to summer 2018. Fortunately, this testing can be done in parallel with testing of the small-scale specimens of the gusset-less connection.

Figure 1: Example Weld Specimen

Due to the focus on the fatigue testing in the small-scale connection during this quarter, the testing on the weld specimen was not performed in the third quarter of 2018 and it is planned to happen next quarter. The grips from Material Testing Technology (MTT) are still available for the test.

Analytical Models of Small-scale Physical Specimens

This task was completed in the first quarter of 2018.

Fatigue Testing

<u>Test Setup</u>
The fatigue testing of Specimen A has been carried out during this quarter. A total of 1.3 million cycles have been applied to the specimen and damage has not been detected. The plan is to test the specimen up to 1.6 million cycles.

The original test setup was evaluated by applying several monotonic load tests to characterize the behavior of the entire system. Based on these initial tests, modifications were made to the setup to create a more stable system in which the relative ratio of the rigidity of the supports, including their attachments to the strong floor, to the rigidity of the specimen increased. The most relevant changes included the following; pouring concrete inside the reaction frame to add stiffness, lowering the actuator to reduce stress concentrations on the vertical attachment plate on the actuator side, adding a support under the tip of the specimen to prevent lateral loading on the actuator, and adding shims under the bracket and reaction frame to compensate for uneven sections of the floor under the test configuration. The entire setup, in its current (modified) state, is shown in Figure 2.

Figure 2: System Components - (Left to Right) Overall Test Setup, Reaction Block (a), Bracket Support (b), Specimen (c), and Shim Support (d)

In addition to the physical test setup, a loading protocol was also developed for this test. The fatigue loading that is being used in this test is a pulsating tensile loading, in which, the actuator is cycling in force control as a sinusoidal signal in tension. The loading specifications are as follows:

- Mean axial load applied: 55 Kip (244.7 kN)
- Cyclic amplitude: ±50 Kip (222.4 kN)
- Cyclic frequency: 3.5 Hz
- Applied function: Sine wave
- Cycles per Test Session: Fatigue = 25600 cycles, SI = 200 cycles

The level of loading was limited by the capacity of the actuator, which is 110 Kip (489.3 kN), while the frequency of loading was limited to consider the test "quasi-static".

<u>Instrumentation</u>

The objectives of the experiment must be considered prior to determining the location and type of sensors. Each sensor should provide a needed piece of information to fulfill these objectives. For this experiment, the bridge owner was interested in (1) investigating the design assumption of fatigue category C for the gusset-less truss connection, which implies infinite-fatigue life under service conditions, and (2) collecting data useful to provide guidance for fatigue-focused visual inspection procedures of the gusset-less connection through the service life of the bridge. The research team was also interested in verifying the structural model of the gusset-less connection and evaluating the dissipation of strain with distance from the weld toe. In order to accomplish these goals, the experimental set up, including boundary condition and component interface, must be categorized and fully understood for both fatigue assessment and structural model verification.

The measurements techniques and sensors that are utilized for the scale model laboratory fatigue experimental are DIC, LVDTs, and strain gauges (uniaxial and rosettes), which are used to measure displacements, rotations and strains. The instrumentation used can broadly be categorized as contact (LVDTs and strain gauges) and non-contact (DIC) measurements.

Strain gauges and LVDTs are two of the most traditional contact tools for obtaining structural response measurements. These sensors function by maintaining contact with the specimen, through contact in the case of the LVDT, or bonding (epoxy or spot-weld), in the case of the strain gauge. These tools tend to be the most commonly used due to their cost, availability, reliability, and accuracy of structural response measurements. Although strain gauges are the most frequently used sensors, there are some significant drawbacks and limitations to their use and applicability. One of the most significant drawbacks for the strain gauges is the installation procedure, which generally consists of the following: 1) surface preparation (sanding/grinding and cleaning), 2) positioning of gauge, 3) application of adhesive and gauge placement, 4) wiring configuration (solder if necessary), 5) connection to strain measuring device and data recording. Strain gauges are limited to relatively smooth and preferably flat surfaces that allow complete bonding of the gauge to the specimen. Additionally, the locations that the strain gauges and LVDTs can be installed is limited to locations that can be physically accessible with sufficient space to perform all the steps necessary for installation.

Another major drawback to these contact measurements is the amount of surface preparation required for adequate installation. Not only is surface preparation a significant amount of work but it also has the potential to interact and affect the specimen behavior. Specifically, if there is any coating or outer layer of environmental protection on a specimen, the surface preparation requires coating removal, while this is not an issue for laboratory specimens exposed to indoor environmental conditions, it can adversely impact field application. Further, strain gauges and LVDTs only provide discrete measurements at the point of installation. Often times, the amount of measurements needed to fully characterize the response of a specimen is significant. To capture all the required measurements, many sensors are necessary, which is costly in terms of number of sensors and installation time. To a lesser extent, the size of these sensors may also provide important limitations, especially when localized strain measurements are needed very close to one another.

The DIC measurements fall under the non-contact measurements category since contact is not present between the cameras and the specimen. DIC identifies and tracks the movement of groups of pixels captured via a speckle pattern on the area of interest. Using a correlation algorithm, the translation vectors for each pixel grouping are calculated and the movement is computed relative to the location of the pixel groupings of an undeformed reference image. Although DIC is not as widely used as the traditional measurement methods, it is becoming more popular as digital image technology advances become more cost-effective and the post-processing technology improves. DIC measurements, while not being as consistently accurate as traditional methods given the impact of image collection conditions and camera capability, excels in many other aspects. One of the largest benefits of DIC compared to other forms of instrumentation is its ease of installation. DIC requires very little installation time depending on the type of equipment used and the environment where the measurements are collected. The general installation procedure is as follows: 1) application of a suitable tracking pattern to the measurement area, 2) placement of camera(s) to focus on the measurement area, 3) adjustment of camera settings to optimize focus, lighting, and resolution, 4) data recording. An experienced user can record measurements with DIC in a relatively short time without difficulty. The other major benefit is that the DIC measurements can be used to characterize a large area where applying multiple gauges would not be feasible. With the correct setup and equipment, it is possible to obtain a full-field characterization of the area of interest. Lastly, the initial cost of the DIC equipment can be high, but it is a tool that can be reused and applied to a variety of situations, which has the potential to mitigate long-term costs.

The strain gauge instrumentation plan for the specimen is shown in Figure 3. In this study, a total of 12 strain rosettes and 10 uniaxial strain gauges are being used to characterize the strains throughout the specimen, especially the strain field near the radiused fillet weld at the web-flange intersection. For this reason, strain rosettes are installed on both sides of the specimen web at three locations along the curved geometry (NRW1/SRW1, NRW2/SRW2, NRW4/SRW4 in Figure 3) and aligned at three distances from the toe of the weld (NRW2/SRW2, NRW3/SRW3, NRW5 in Figure 3) to capture the strain distribution in the web. Additionally, three rosettes are placed on the top flange; two on the underside (NRFB1/SRFB1) and one on the topside (SRFT1) to characterize the strain in the flange. The uniaxial gauges are placed on the specimen close to the interface between the specimen and its boundary conditions, specifically the actuator and the bracket support (NU1 to NU6; SU2, SU5; VP1, VP2 in Figure 3). These uniaxial gauges are in place to measure the structural response at the interfaces and provide data useful for characterization of boundary condition effects. These measurements can also be used to calibrate a numerical model of the test setup. Additionally, DIC is used to take measurements in the blue hatched area shown in Figure 3. The DIC serves as a verification for the strain rosettes as well as a full-field characterization in this region at locations in which strain rosettes are not present.

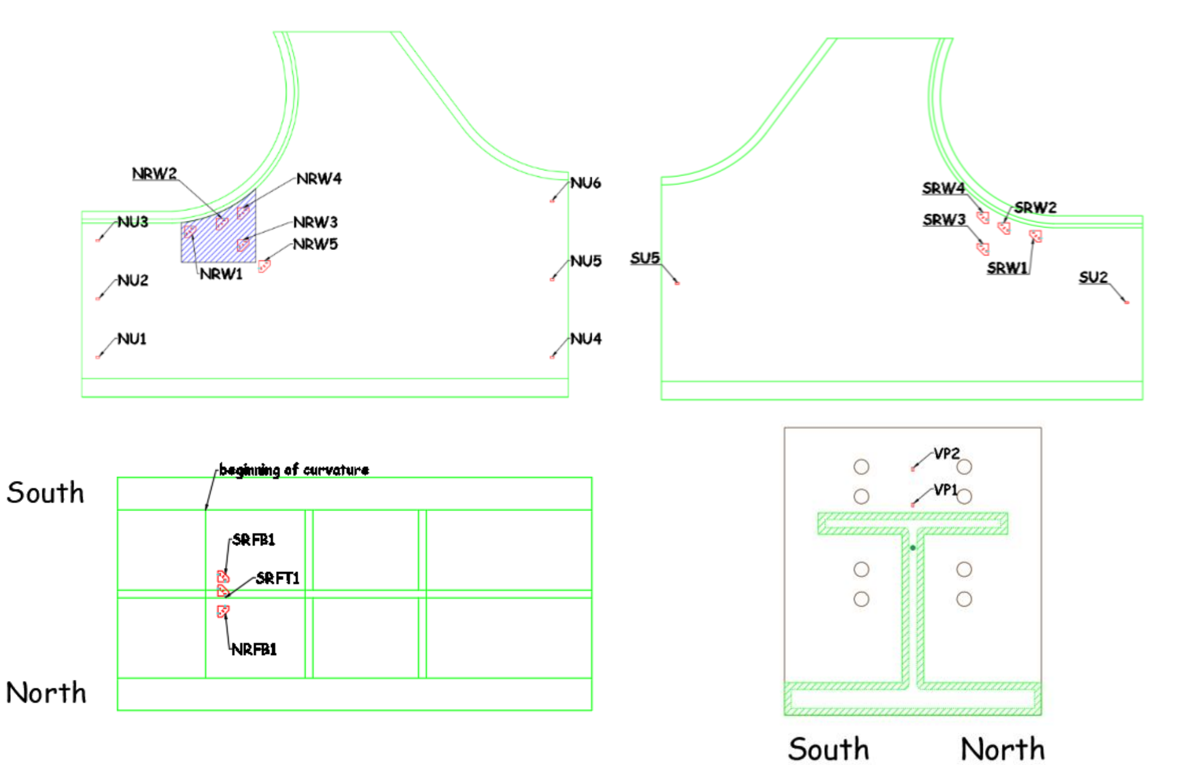

Figure 3: Strain Gauge Instrumentation – (left to right) North Elevation, South Elevation, Plan View, and East Elevation. DIC area of interest is depicted by the blue hatched area

<u>System Identification</u>
The system identification (SI) refers to a full characterization of the structural response of the test setup being investigated. The SI serves two purposes: (1) ensuring the test is producing measurements in the expected range, and (2) monitoring and verifying the consistency of the structural behavior throughout the fatigue test prior to specimen damage.

In the current experiment, high cycle fatigue testing is performed since the level of stress is estimated to be approximately 47% of the yield stress at the critical location and the expected number of cycles is greater than 10^5; therefore, the fatigue test is expected to be completed over multiple testing periods. The test is performed under constant loading (force) amplitude and it is expected that the specimen will experience a consistent range of stress, which can be verified, for example, by evaluating the strain history measurements collected during the test. The stability and consistency of the testing environment and boundary conditions is critical during the test. Consequently, it is critical to characterize the behavior prior to the test. Any changes in the test setup during the test could result in system responses that are inconsistent. Using the SI, a reference set of measurements is generated to serve as benchmark for future characterizations of the system. Using this benchmark as a reference, the system will be periodically checked with a SI to ensure that the behavior is consistent between fatigue cycles.

In addition to the instrumentation described in the previous section and shown in Figure3 DIC is used at key locations identified in Figure 4 with a red hatch pattern. These locations were chosen to characterize the boundaries between different portions of the test setup, as well as acting as verification points for additional measurements made with the LVDTs, which are not shown in Figure 4. The locations of the LVDTs are not fixed, as they are the easiest measurement method to move; therefore, they are moved between SI sessions to provide different verification locations. All measurements are taken simultaneously during each SI session.

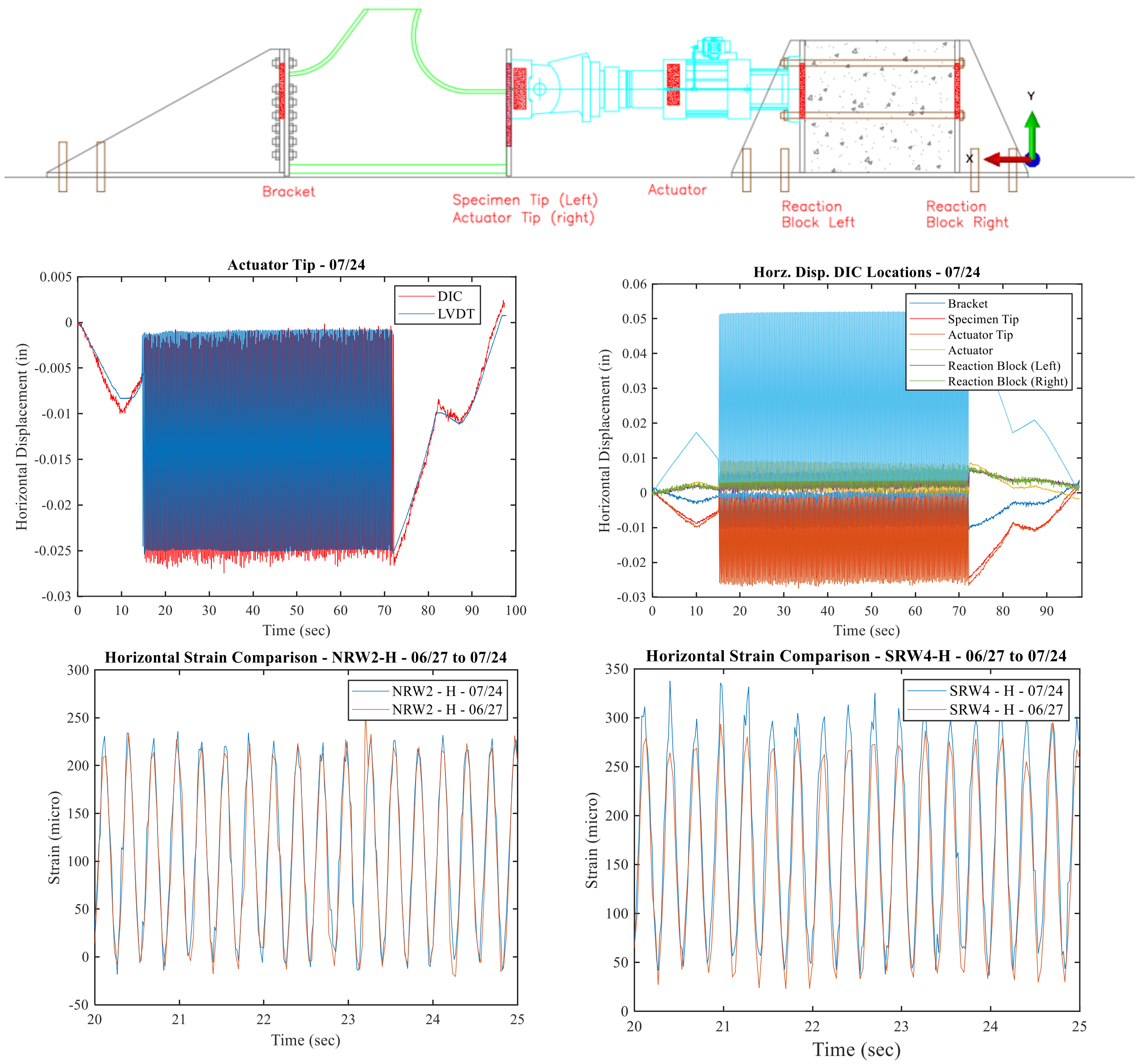

Figure 4: SI (left to right) - DIC Captured Locations, DIC vs LVDT Verification, DIC Horizontal Disp. of System, Strain Comparisons - 06/27/2018 to 07/24/2018

The naming convention of the data sets correspond to a specific day in which a test and/or SI was performed, therefore 06/20 refers to June 20th, 2018.The plots in Figure 4 shows some of the measured results from the SI performed on 07/24. The first plot shows the comparison of the horizontal displacement measured at the level of the actuator from the DIC and an LVDT in contact with the vertical plate of the specimen. Based on these results as well as results from other comparison locations, it is shown that the two measurements are consistent with one another and therefore act as verification for each other. The next plot shows the horizontal displacements at a consistent elevation from each DIC capture location in the system; these measurements serve as a benchmark to evaluate potential changes in boundary conditions for future SIs. The final two plots show a comparison between the strain measurements in the strain rosettes at different instances during the testing. The first measurement is from a SI on 06/27 and it is being compared to a SI from 07/24. The left plot shows that even though the system had been changed between the two dates, it was not reflected in this strain gauge (NRW2-H), while the right plot reflects a clear change in the recorded measurements between the two dates. This indicates that monitoring the system through the strain data alone would not sufficiently capture changes in behavior, which highlights the importance of performing a SI to capture the overall response of the test setup.

Lastly, the loading protocol of the SI is identical to the one used during the fatigue test except for the number of cycles. If SI calculations show significant changes that are not associated with potential specimen damage at some instances during a fatigue test, corrective action ought to be taken (e.g., tightening of the nuts used to anchor the supports to the strong floor via anchor threaded rods).

Monitoring and Test Setup Refinement

Ensuring consistent behavior in a prolonged test is important but performing a SI before every testing period would be cumbersome and would add a significant testing delays. Hence, it is important to have the availability of benchmark measurements during the fatigue test that could be used as reference measurements to identify potential undesirable changes in the structural response of the system. Having such measurements allows the test to be monitored between SI intervals and can be used as a tool to decide when an additional (unscheduled) SI needs to be performed.

In this study, the measurement that is being used as a representative characterization of the system is the force-displacement relationship of the actuator. The force-displacement relationship is an indicative measurement because when applying a consistent force (force-controlled test), any change in a stable system, for example boundary conditions, will be reflected in this measurement. If there is a noticeable change in the force-displacement hysteresis of the actuator, the test setup ought to be evaluated for changes in the supports, any loosening of bolts, or any noticeable damage. If the source of the change is not visible, a full characterization is required in the form of the SI process. This creates a systematic approach for maintaining a consistent structural response throughout the fatigue test.

Throughout this study, a history of the force-displacement relationship has been monitored to create a benchmark measurement and use this benchmark to assess the presence of changes in the system. Figure 5 shows a history of the force-displacement relationship of the actuator throughout the setup testing phase of this project. It is important to note that the data shown includes ten load cycles close to the end of the test period for each data set. The naming convention used is the same as the one described in the previous section.

The first data set, 06/20, was the first fatigue test period. After, inspecting the test setup, minor grinding of the concrete floor was observed under the vertical attachment plate to the actuator. Therefore, the supports were modified from narrow steel channels to flat aluminum shims to mitigate this grinding. The objective of this change was to increase the surface area of the support to distribute the force and allow for the shims to slide on each other rather than the channel grinding against the concrete floor.

The next data set was from 06/27, which was a SI study to characterize the system with the new supports. The force-displacement from that data set shows a significant reduction in the slope from the previous test, which is attributed to the change from the steel channel to the aluminum shims. With this change, the specimen was able to displace further under the same load since the aluminum support was much more flexible. During this SI session, it was noted that the reaction block, which supports the actuator, was rotating about the z-direction and moving horizontally, so a decision was made to increase the torque applied to the anchors that clamp the reaction frame to the floor. This resulted in an increase in overall stiffness, shown from the 07/03 data set. This is due to the actuator previously having to displace more to achieve the same level of force, therefore, when the support was sufficiently restrained to the floor, the actuator did not have to compensate for any additional movement.

Data from 07/07 and 07/10 (Morning) shows a slight loss of stiffness in the force-displacement relationship. In both tests, the shim supports under the vertical plate became dislodged from their initial location. Both tests were stopped before reaching the desired level of cycles to make adjustments to the support and improve the boundary conditions. This change in behavior was critical to prove that the force-displacement relationship is an effective measurement tool to identify undesirable changes in the system. The results of the changes are reflected in the data of 07/10 (Afternoon). Between 07/10 (Afternoon) and 07/11, the only change to the system was re-applying the correct torque to the anchors of the entire system. This resulted in a slight increase in the slope of the force-displacement relationship, indicating a slight increase in stiffness. It was also noted that the vertical displacement of the shim support under the vertical plate was visually larger than previously seen. Therefore, the aluminum shims were replaced with steel shims, which is reflected in the data set from 07/16. Following 07/16 no system changes were made, only the bolts were checked for the proper torque setting.

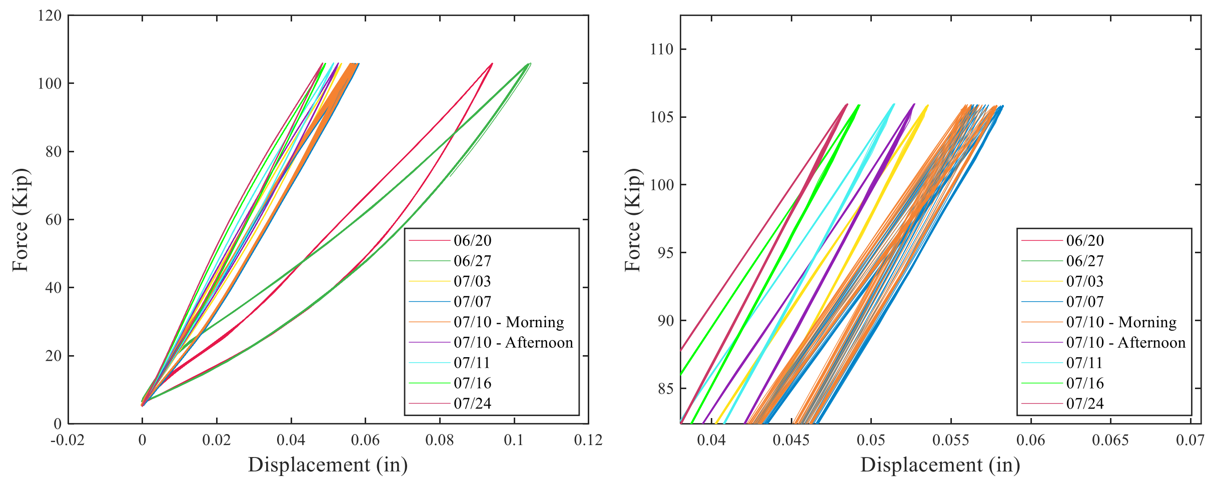

Figure 5: Actuator Force-Displacement Histories

Preliminary Test Results

This section provides an overview of preliminary strain data from the strain rosettes and the DIC during cyclic loading in the area of interest, near the radiused fillet weld, including verification of the accuracy of measurements obtained using the DIC. The strain shown from the gauges is the total strain induced by the combination of the application of the load during the protocol and the installation of the specimen in the test setup, i.e., the strains induced by the installation process are not adjusted to zero before the fatigue test. Figure 3 shows the referenced locations for the strain rosette data as well as for the DIC area of interest, which is shown hatched in blue.

The measured strains from the strain rosettes in the area of interest show that the highest strain range during cyclic loading on the North side of the specimen is measured from the ‘NRW4’ gauge in the horizontal direction. The measured strain ranges from approximately -10 $\mu\epsilon$ to 270 $\mu\epsilon$ for a total range of approximately 280 $\mu\epsilon$, where negative values denote compression and positive values tension. After identifying this as the highest measured strain using the strain rosettes, an area close to the gauge, indicated as ‘DIC-Verification’ in Figure 6 was investigated using DIC in order to verify the measurements against one another. Figure 6 shows the two (unfiltered) measurements are very similar in magnitude, with only slight variations that can be attributed to noise in the measurements, caused by digital image artifacts, as well as the limitation of the DIC sample frequency. The captured frequency is limited to 20Hz with the data acquisition hardware used, and therefore the collected data does not always capture the peaks and valleys of the response. This comparison, which has been performed at multiple locations (not shown here for brevity), provides confidence in the accuracy of the measurements from the DIC. Further, the DIC was used to measure the strain at locations, depicted as the yellow line in Figure 6, next to the weld (noted by the green region), to obtain a better characterization of the stresses and strains that the weld is being subjected to. Based on these measurements the highest measured strain in this field of view occurs at the point identified in Figure 6 with an orange ‘X’. The horizontal strain range that is measured at this location is estimated at 420 $\mu\epsilon$, which is approximately 50% greater than the highest strain range measured from the closest strain rosette. This reinforces the importance of measurements closer to the actual weld geometry, which is the most critical area of interest in this fatigue study.

Although not shown in the figures, there is a difference of approximately 50 $\mu\epsilon$ between the North (N) and South (S) side strain measurements obtained from strain rosettes that are opposite to each other. The magnitude of the strain measurements from the South side strain rosettes are consistently higher. This is most likely caused by the shims, shown in Figure 2, providing support to the specimen under the vertical plate connecting the specimen to the actuator and constraining the torsional response of the vertical plate at this location. Due to manufacturing imperfections on this plate as well as the floor not being perfectly level, there is a slight rotation in the specimen about the longitudinal axis of the actuator. Despite this difference in the magnitude of strains, the stress ranges are similar, with an average 6 με difference in the range, so fatigue performance should not be significantly impacted. The magnitude of the rotation is being characterized by LVDTs during the SI. Quantification of this rotation is also important so that this information can be incorporated into the numerical model to better simulate the response.

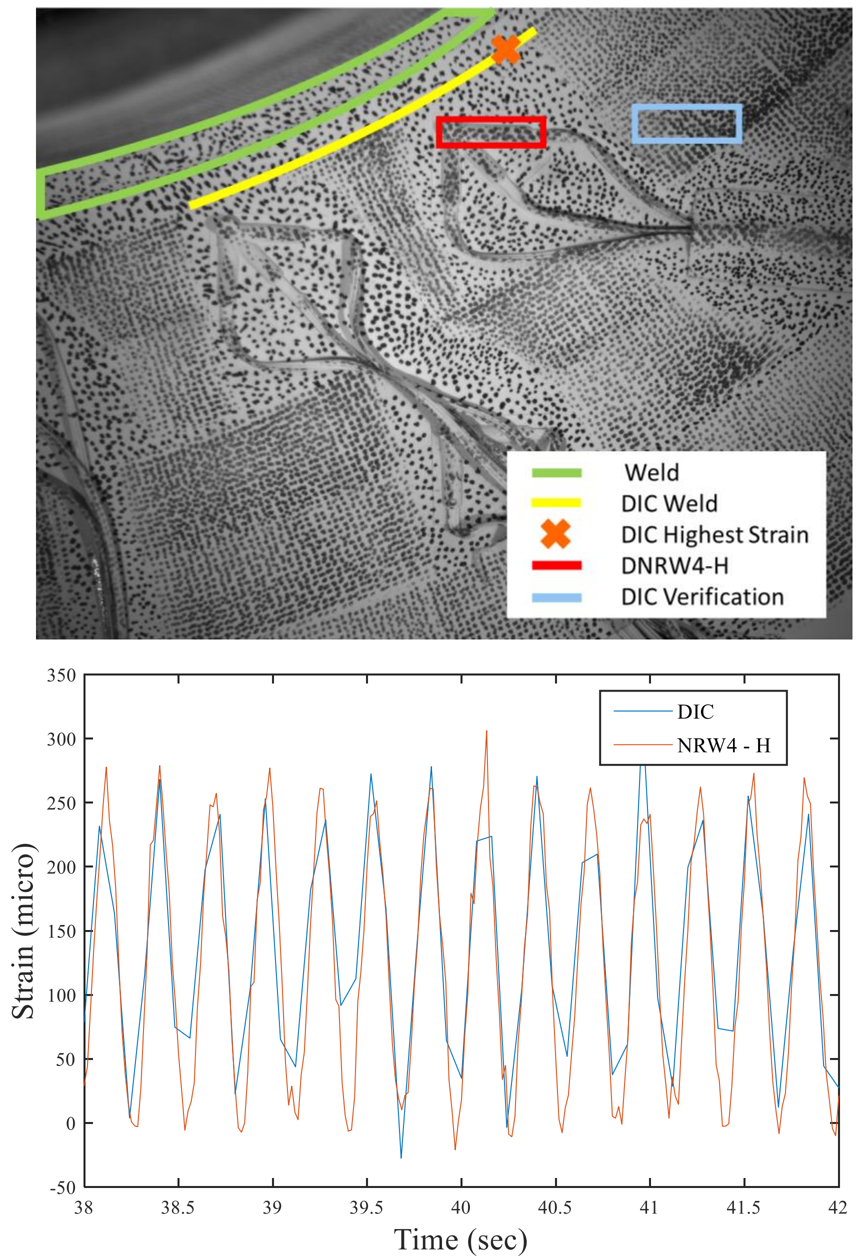

Figure 6: DIC Field of View, DIC vs. Strain Rosette - Horizontal Strain Verification, DIC near the Radiused Fillet Weld

Numerical Model

In this study, a finite element model (FEM) of the specimen as well as portions of the test setup was developed using ABAQUS® CAE/2017. The model was created in order to estimate stresses and strains in the specimen as well as the overall structural response of the test setup. The results of the finite element analysis (FEA) are compared to the actual measurements from the test to conduct model calibration.

The FEM, shown in Figure 7, consists of four main parts: actuator swivel, specimen, bracket, and rigid floor. The connection specimen consists of the vertical attachment plate on the actuator side, the front top flange, the web, the bottom flange, the back top flange, and the vertical attachment plate on the bracket side, which are welded to each other. The various components were modeled and meshed using C3D8R elements (solid reduced integration linear brick elements) and C3D10 elements (A 10-node quadratic tetrahedron). These components are connected by the weld surfaces with a tie interaction. In addition to this, interaction between the individual parts, excluding the weld, is modeled with surface-to-surface contact. This interaction was chosen to simulate the most realistic transfer of stresses through the specimen, which would be through the weld itself or via contact between the various components of the model at their intersections. Moreover, the bolted connection of the specimen to the actuator swivel, as well of the specimen to the bracket, are simulated in the numerical model. The bolt's interactions with each individual component are modeled as surface-to-surface contact. This method was chosen to simulate the interaction between parts including their potential separation or loss of contact, whereas the tie constraint would simulate the components working as a unit. Lastly, the bracket has a frictionless, "hard" contact, interaction with the rigid floor.

The boundary conditions of the FEM were chosen to be representative of those present in the experimental test setup. Boundary conditions are applied at four locations in this FEM; the swivel's center of rotation, the bottom surface of the vertical attachment plate on the actuator side, the surface of the rigid floor, and the locations of the anchor holes in the bracket. The actuator swivel is restrained from rotation about the X, Y, and Z directions and allowed to translate in the X, Y, and Z directions. These restraints were selected to simulate the swivel, which has its orientation locked in place, preventing any rotations during loading. The bottom surface of the vertical attachment plate on the actuator side is restrained from rotation about the Z direction and restrained from translations in the Y direction. These restraints are representative of the metal shim supports that are under this vertical plate, these shims slide on top of each other while restraining any vertical (Y direction) movement and preventing rotation. The bracket is restrained from translations and rotations at the location of the anchors. This is meant to simulate the near fixed-end condition created by the four anchors at the end of the bracket. Lastly, the rigid floor is restrained in all directions against translations and rotations to simulate the actual floor under the test setup.

The loading protocol is implemented in the numerical model in two steps; the pre-tensioning step, and the static loading step. The pre-tensioning step is created to simulate the application of the bolt loads generated from tightening the bolts that connect the various components together as discussed previously. These loads create a clamping axial force on the two connection components that is meant to be consistent with the actual axial force applied to these bolts. This force was estimated by applying a known torque (800 ft-lb or 1085 Nm) to the bolts and converting the torque to an axial force which was then applied to each bolt in the FEM. In the static loading step, a 100 Kip (445 kN) ramp tension load, is applied to the actuator swivel. The load applied is equivalent to the loading range applied to the specimen during a fatigue test, from a minimum of 5 Kip (22.2 kN) to maximum of 105 Kip (467 kN).

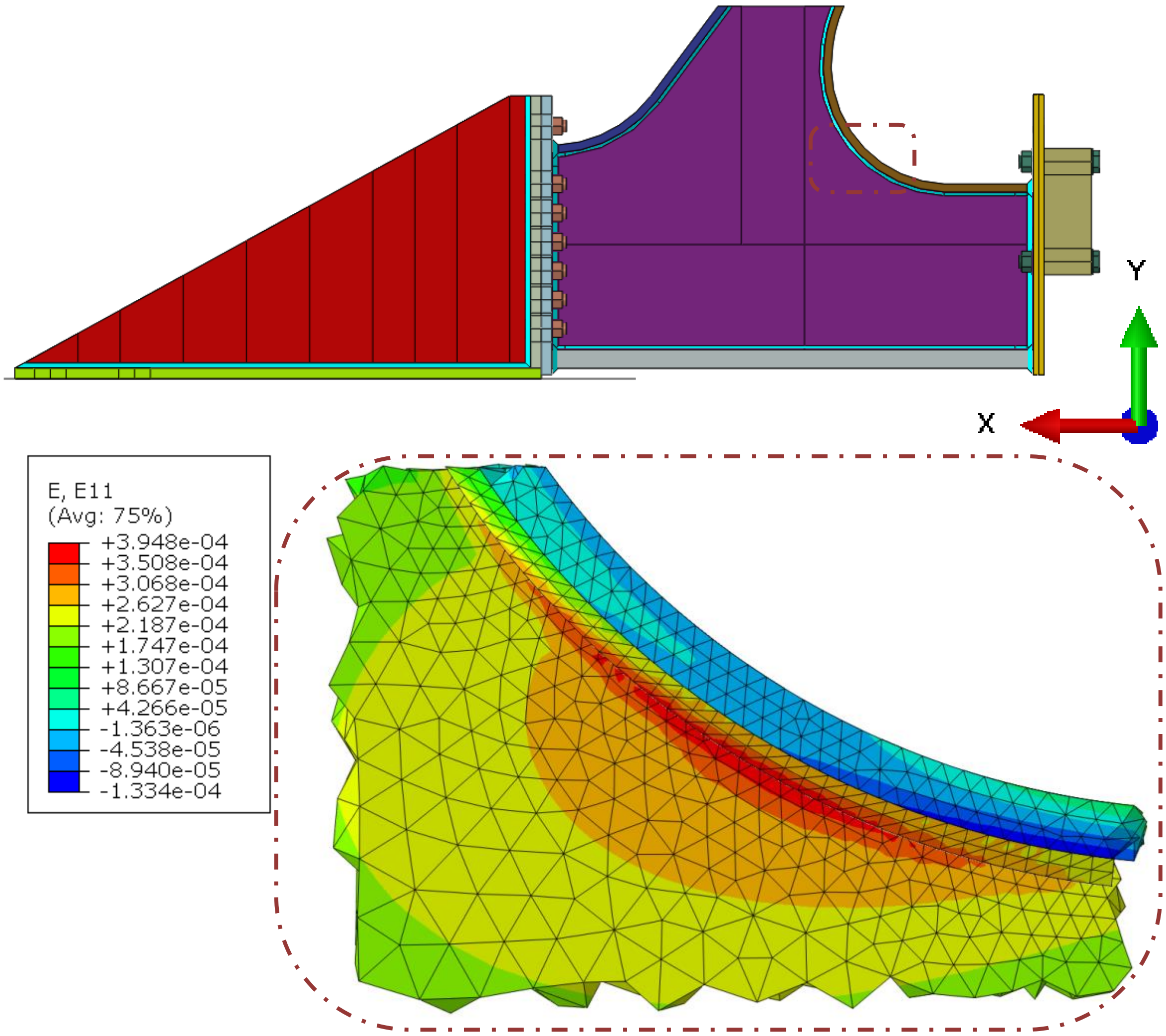

Figure 7: FEM Assembly and Orientation (Top), Horizontal Strain in Area of Interest (Bottom)

Using the aforementioned loading protocol, the resultant strain contours are shown in Figure 7 (Bottom). The strains obtained from the numerical model can be compared to the measurements from specimen and test setup. Once the model has been verified, it can be used to estimate stresses and strains in the radiused fillet weld itself as opposed to directly adjacent to the weld. This analysis will help supplement the information obtained from measurements as only strain data adjacent to the weld can be obtained experimentally.

With this limitation in mind, a combination of DIC and strain gauge measurements were used for verification purposes around the area of interest. Specifically, the four strain rosettes on the North side closest to the weld (Figure 2, NRW1-4) were compared to elements at the same location in the FEM. Additionally, the measurements obtained through DIC are also compared to measurements from the FEM. A summary of this evaluation is shown in Table 1.

Table 1 - Horizontal Strain Evaluation - Numerical vs. Measured.

Location	Strain Range (με)		Percent Difference (%)
	Measured	Numerical	
NRW1	215	230	7
NRW2	270	285	5
NRW3	200	212	6
NRW4	280	289	3
DIC 1	280	324	14
DIC 2	295	300	2
DIC 3	385	367	-5
DIC 4	420	376	-12

These values indicate that the response of the FEM closely represents the measurements being obtained from the actual specimen. Although the exact values of the highest strain are not identical, the overall strain magnitudes are relatively close to one another. The highest difference noted from the DIC measurements was 14%, which is equivalent to 44 με. This variability is relatively high but expected due to the noise, previously mentioned, in the DIC measurements. Of the strain gauge measurements, the highest difference was 7%, which is equivalent to 15 με. Based on these results the stresses in the weld, calculated with the numerical model, should be reasonably close to what the actual specimen is experiencing. The highest stress in the weld from the model is approximately 23.7 ksi (163.4MPa).

Coupon Tests

For material characterization, coupon specimens were fabricated at UNH Machine Shop from the same batch used to fabricate the web and the flanges of the specimens. These tests will be conducted under tensile load at the Instron Machine. The plates for the tensile test were provided by CANAM Bridges.

Residual stresses

To better characterize the stress state of the connection, residual stress tests have been performed. The residual stress tests have been performed prior to testing and are being performed during testing using a blind-hole analysis. This means that the specimen is fitted with a specialized strain rosette and a small-diameter hole is incrementally drilled into the specimen to a specified depth (see Figure 8). This drilling relieves the stresses around the hole, which results in strains measured by the strain rosette. These strains can be mathematically related to the total stresses that were present in the specimen before drilling. Due to the unique fabrication of this specimen, it is deemed important to quantify the residual stresses due to the cold-bending process, and the residual stresses around the weld area. In order to have a reasonable benchmark, a residual stress test was also performed on a plate of the same material that did not undergo any bending or fabrication. Additional post-processing of these results has been conducted in this quarter.

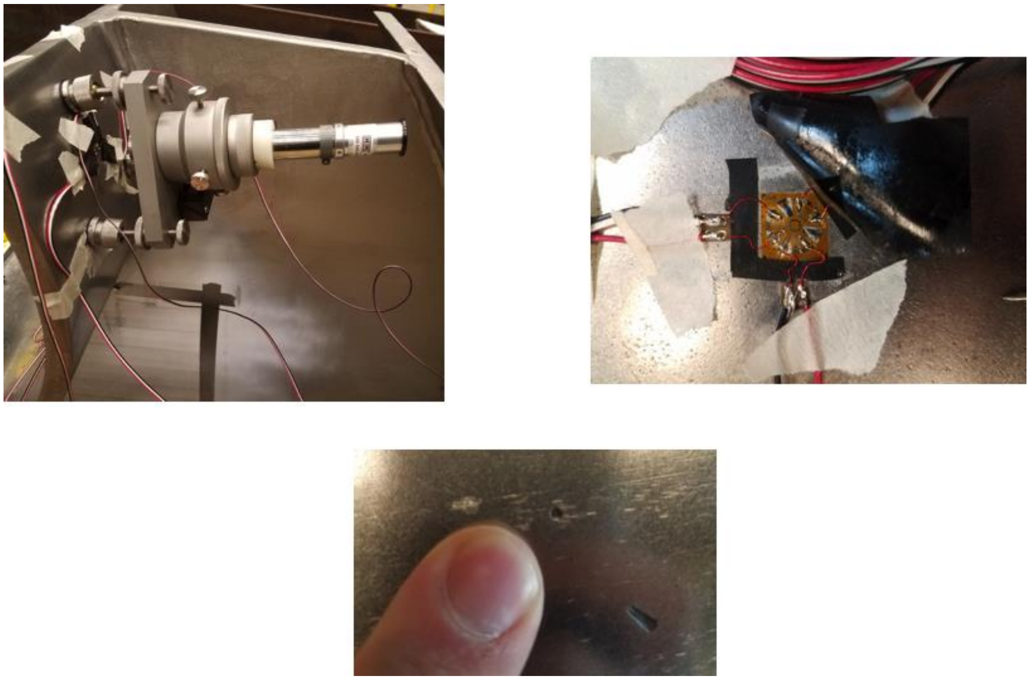

Figure 8: Residual stress test (a) drill rig, (b) strain rosette, (c) 1/8" diameter hole.

Evaluation Protocol for Inspection and Condition Assessment
There was no progress on this task during this reporting period.

Final Report and Presentation
There was no progress on this task during this reporting period.

Meetings
A TAG meeting was held at the NHDOT offices in Concord, NH on September 27, 2018 to update the NHDOT on the research activities and solicit their input on the remaining research tasks. Dr. Bell (PI), Dr. Medina (co-PI), Duncan McGeehan (graduate student) and Shokoufeh Zargar (graduate student) participated in this meeting from UNH.

Dr. Medina, Dr. Bell, Duncan McGeehan, Shokoufeh Zargar and Maryam Mashayekhizadeh (graduate student) had a conference call with Ted Zoli and Christopher Engel at the HNTB offices to discuss various aspects of this project, especially some of the details related to future fatigue testing activities that could be part of future projects depending on the results of this research effort in September 2018.

Items needed from NHDOT (i.e., Concurrence, Sub-contract, Assignments, Samples, Testing, etc):

There are no items needed from the NHDOT at this time.

Anticipated research next 3 months:

Complete the fatigue testing of weld samples with the new grips on the universal testing machine at the structural high bay and testing of Specimen A. As part of the September 2018 TAG meeting, the possibility of testing Specimen A after damaged has been induced to both sides of the radiused fillet weld was discussed. The objective would be to understand crack propagation and the redistribution of stresses in the connection area if a crack were to develop. Testing Specimen A after damage has been induced to the radiused fillet weld and testing of Specimen B would most likely have to be part of a second project phase. In addition, the final report will be prepared during this quarter.

Circumstances affecting project: Describe any challenges encountered or anticipated that might affect the completion of the project within the time, scope, and budget, along with recommended solutions to those problems.

As described in the previous quarterly reports, delays associated with specimen fabrication, the need to modify the Instron Universal Testing Machine at UNH, the receipt of defective grips for fatigue testing of weld specimens, technical issues relating to the data acquisition system at the Memorial Bridge have negatively affected the schedule of this project.

Tasks (from Work Plan)	Planned % Complete	Actual % Complete
Evaluation of Gusset-less Truss Connection to Aid Bridge Inspection and Condition Assessment		
Literature Review and Finalize Testing Plan	**100**	**100**
Design and Construction of Small-scale Models	**100**	**100**
Quasi-Static Testing to Failure – Replaced by Load Test of the in-service connection at the Memorial Bridge	**100**	**100**
Validation of Structural Connection Analytical Model	**100**	**100**
Fatigue Testing	**100 (for Specimen A)**	**80**
Data Analysis and Interpretation of Laboratory Testing	**75**	**60**
Evaluation Protocol for Inspection and Condition Assessment	**0**	**0**
Final Report and Poster	**0**	**0**